Influence of Cerium(IV) and Bismuth(III) on the Luminescence Properties of the Nanocrystalline Hydroxyapatite

ANA MARIA BARGAN (MATEIUC), GABRIELA CIOBANU*, TEODOR MALUTAN, CONSTANTIN LUCA
"Gheorghe Asachi" Technical University of Iasi, Faculty of Chemical Engineering and Environmental Protection, Department of Organic, Biochemical and Food Engineering, 63 Dimitrie Mangeron, 700050, Iasi, Romania

Cerium(IV)- and bismuth(III)-substituted hydroxyapatite nanoparticles were synthesized by the co-precipitation method from aqueous solutions of various Ce/(Ce+Ca) = X_{Ce} or Bi/(Bi+Ca) = X_{Bi} atomic ratios ranging from 0 to 0.5. Samples were characterised by scanning electron microscopy (SEM) coupled with X-ray analysis (EDX), X-ray powder diffraction (XRD) and fluorescence spectroscopy. The luminescence characteristics of the Ce^{4+} and Bi^{3+} ions in the hydroxyapatite lattice have been studied under the $\ddot{e}_{exc}$ = 300 nm. The results obtained from the fluorescence spectra revealed that the optical properties of the hydroxyapatite samples are modified by the substitution with cerium or bismuth ions.

Keywords: hydroxyapatite, cerium, bismuth, optical properties, luminescence

The hydroxyapatite (HA), $Ca_{10}(PO_4)_6(OH)_2$, well known for its excellent bioactivity, biocompatibility and osteoconductivity, is one of the most important calcium phosphate based bio-ceramic materials [1-4]. The hydroxyapatite crystallizes in the hexagonal system with $P6_3/m$ space group. The literature reports demonstrate the flexibility of the apatite structure as regards the substitution with other different cations in the "Ca" sites such as monovalent (Na^+, K^+), divalent (Sr^{2+}, Pb^{2+}, Ba^{2+}, Mn^{2+}, Cd^{2+}, Mg^{2+}, etc.), trivalent (Cr^{3+}, Al^{3+}, Fe^{3+}, rare earths ions REE^{3+}, etc.), tetravalent (Ti^{4+}, Th^{4+}, U^{4+}) and even hexavalent (U^{6+}) cations. These substitutions can improve the physical, chemical and biological properties of HA [5].

The idea to produce a luminescent agent of a great biocompatibility is ideal for implantation and clinical applications [6, 7]. The biomaterials with excellent optical properties were intensively studied in the last decade due to the increasing demand for efficient light-sensitive materials not only for the optoelectronic and photonic devices, but also for a broad range of applications in the biomedical field. In particular, the researches were directed to the use of the hydroxyapatite as drug-delivery vehicles that can target tissues or cells [8] and can be functionalized with special characteristics (such as magnetization, fluorescence, and near-infrared absorption) for qualitative or quantitative detection of tumor cells [9].

Lanthanides (La, Ce, Nd, Sm, Eu, etc.) display fascinating optical properties. Among the applications of luminescent lanthanide ions the following can be cited: (1) their continuing use in lighting industry for the engineering of lamp and display phosphor, (2) their ability to provide electroluminescent materials for organic light-emitting diodes as well as optical fibres and amplifiers for telecommunication, (3), their potential in the design of luminescent liquid crystals, and (4) their capacity to yield functional complexes for biological assays [10].

Besides, the bismuth is one of the most investigated elements, being regarded as "the wonder metal" because of its diverse oxidation states. Its behaviour as smart optically active centres in diverse materials has been noticed in the last decades [11-14]. Due to these properties the bismuth compounds have important applications in areas of telecommunication, biomedicine, white light illumination and lasers. Webster et al. [15] reported that the Bi^{3+} would be the best choice of dopant to enhance properties of HA pertinent for bone implant applications.

In this work, the preparation and characterization of the Ce- or Bi-doped HA by means of wet chemical method based on co-precipitation reactions is reported. The effects of the Ce^{4+} and Bi^{3+} substitution for Ca^{2+} on the morphology, crystallinity and optical properties of the resulting powders were investigated and discussed.

Experimental part

Materials and methods

All the chemicals were of analytical grade, are used as received without further purification and were supplied by Sigma-Aldrich (Germany). The experiments were performed with triply distilled and deionized water. The undoped HA, Ce-doped HA and Bi-doped HA nano-powders were synthesized co-precipitation method described in our previous works [16, 17]. Method consists in a drop-wise addition of phosphoric acid (0.1 M) to a suspension of calcium hydroxide and cerium or bismuth source (0.167 M), under stirring according to the reactions bellow:

$$(10-x)Ca^{2+} + xCe^{4+} + 6PO_4^{3-} + 2OH^- \rightarrow \rightarrow Ca_{10-x}Ce_x(PO_4)_6(OH)_2\downarrow \quad (0 \le x \le 10) \quad (1)$$

$$(10-x)Ca^{2+} + xBi^{3+} + 6PO_4^{3-} + 2OH^- \rightarrow \rightarrow Ca_{10-x}Bi_x(PO_4)_6(OH)_2\downarrow \quad (0 \le x \le 10) \quad (2)$$

The (Ce+Ca)/P and (Bi+Ca)/P atomic ratios were kept at 1.67 value, while the Ce/(Ce+Ca) atomic ratio (denoted X_{Ce}) and Bi/(Bi+Ca) atomic ratio (denoted X_{Bi}) in the solution varied between 0.05 and 0.5 as shown in table 1. During synthesis, the *p*H value was adjusted to 10 with NaOH (10M), the temperature being maintained at 60°C and the mixing time of 5 h. The Ca/P molar ratio was maintained at 1.67 as required for obtaining a pure and stoichiometric hydroxyapatite.

After a maturation period of 24 h the precipitate was washed with water to remove the residual impurities. The product resulting by filtration was dried in a vacuum dryer for 24 h at 90°C and then calcined at 800°C for 2 h.

* *email: gciobanu03@yahoo.co.uk*

Sample	Synthesis solution			Final product		
	$\frac{X}{X+Ca}$	$\frac{X+Ca}{P}$	X (%)	$\frac{X}{X+Ca}$	$\frac{X+Ca}{P}$	X (%)
HA	0	1.677	0	0	1.673	0
HA-Ce-5	0.05	1.677	5	0.048	1.669	4.8
HA-Ce-15	0.15	1.677	15	0.146	1.675	14.6
HA-Ce-25	0.25	1.677	25	0.247	1.671	24.7
HA-Ce-50	0.5	1.677	50	0.486	1.678	47.3
HA-Bi-5	0.05	1.677	5	0.049	1.666	4.98
HA-Bi-15	0.15	1.677	15	0.144	1.671	14.49
HA-Bi-25	0.25	1.677	25	0.244	1.683	24.43
HA-Bi-50	0.5	1.677	50	0.498	1.672	48.2

X = Ce or Bi ions

Table 1
ATOMIC RATIOS OF THE SAMPLES

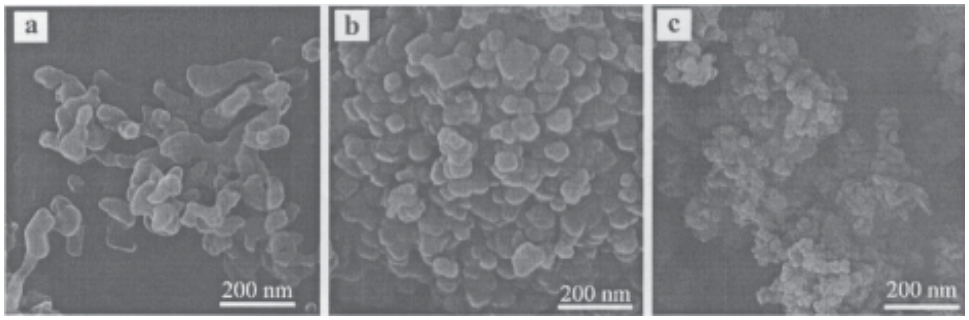

Fig. 1. SEM images of the doped hydroxyapatite samples powders: a) non-doped HA, b) Bi-doped HA, c) Ce-doped HA

The fine powders thus obtained have been characterized by SEM-EDX microscopy, X-ray diffraction (XRD) and fluorescence spectral measurements.

Measurements

The morphology and chemical composition of the sample surfaces were elucidated by scanning electron microscopy (SEM) coupled with energy dispersive X-ray spectroscopy (EDX), with QUANTA 200 3D Dual Beam scanning electron microscope (FEI Co., USA). For the SEM-EDX investigations, gold sputtering was used to create a conductive coating surface. The phase composition, degree of crystallinity and size of crystallites of the samples were estimated by X-ray diffraction analysis (XRD) with X'PERT PRO MRD diffractometer using CuK_α radiation (λ = 0.15418 nm). Fluorescence emissions of the materials obtained were recorded on a spectrometer Perking Elmer LS 50B Luminescence using acrylic cell (10x10x48 mm), a length of excitation 300 nm and emission slits were 5 nm, scan speed 500 nm/min to the absorption domain of 300-600 nm.

Results and discussions

Structure and characterization of cerium-doped HA and bismuth-doped HA

The SEM micrographs illustrated in figure 1 reveal the morphology and size of the samples. It can be seen that the hydroxyapatite powders are composed of nanosized primary particles that tend to form agglomerates with intergranular micropores. The SEM images reveal a decrease of the particles size from about 10 to 60 nm which is indicative of a decline of the crystallite size with increasing Ce or Bi content, in agreement with the XRD data.

The Bi and Ce content in apatite do not result in significant changes; all the samples exhibit the same morphology. When samples are calcined at high temperature (800°C) colour changings can be noticed. HA powder appeared blue in colour whereas yellow-green colour was observed for Ce-doped HA and Bi-doped HA samples. These optical observations could suggest the presence of the cerium and bismuth ions in the apatite lattice.

The SEM-EDX analysis was performed in order to determine the surface elemental composition of the powders. EDX spectra (images not show) display the characteristic peaks of cerium or bismuth. By the SEM-EDX elemental analysis (table 1) the Ca/P ratio for each sample was found to be situated between 1.65 and 1.68 in good agreement with literature data [18]. The mass fractions of different elements in the samples were obtained and the atomic ratios calculated as shown in table 1.

These results indicate that cerium and bismuth ions added to the synthesis solution are incorporated into the hydroxyapatite lattice. The degree of crystallinity and size of crystallites of the hydroxyapatite powders with different Ce/(Ce+Ca) or Bi/(Bi+Ca) atomic ratios were determined by XRD analysis.

The XRD patterns described in our previous works [17, 18], indicate that all the samples have the characteristic peaks in the 2θ regions of 21°–29°, 32°–34°, 39°–41°, 46°–54°, in good agreement with the hexagonal (space group $P6_3/m$) hydroxyapatite phase (JCPDS Data Card 09–0432). For the all substituted samples, a decrease of crystallinity with increasing bismuth or cerium contents is observed. As can see in figure 2, if the Ce/Ce+Ca molar ratio is above 0.25 the crystallite size increase, which could be attributed to different charge compensation mechanisms for

isomorph substitution of Ca^{2+} by Ce^{4+} or Bi^{3+} ions. This analysis made possible a better understanding of the luminescence properties of the sample.

Luminescence properties of Ce-doped HA and Bi-doped HA

The emission spectra of the samples under study are illustrated in figures 3 and 4. The excitation wavelength used in this study is of 300 nm. As expected, all the samples show a broad blue-green emission within visible region. The samples display a very strong emission peak centred at about 422.5 nm at room temperature. This peak can be attributed to the hydroxyapatite signal in the visible domain. This HA luminescence behaviour persists with the addition of Ce^{4+} or Bi^{3+} which confirms the HA matrix effect for all samples.

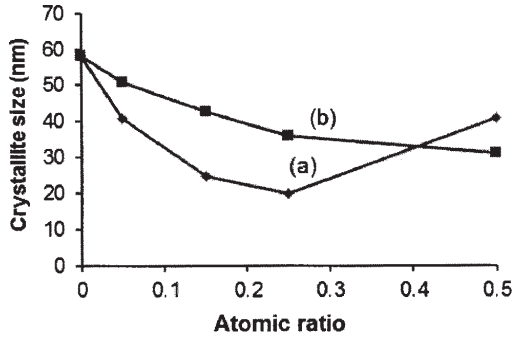

Fig. 2. Crystallite size of the Ce-doped HA samples with different molar ratio of Ce/Ce+Ca (a) and Bi-doped HA samples with different molar ratio of Bi/Bi+Ca (b)

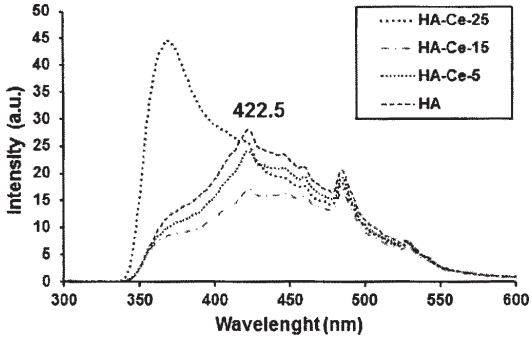

Fig. 3. Emission spectra of the Ce-doped HA at different concentrations

As revealed in figure 3 all the Ce-doped HA samples showed strong visible emission peaks appearing at about 422.5, 447, 460, 485 and 528 nm. The emission intensity of every sample is seen to decrease with increasing cerium concentration till 15% while above this concentration the peak is shifted to shorter wavelengths and higher intensities. This could be explained by the crystallinity decrease of the samples. It is well known that luminescence intensity has a direct correlation with crystallinity [19, 20]. The higher crystallinity, the higher luminescence emission peak is. The HA sample shows a strong green luminescence due to its higher crystallinity while HA-Ce-25 shows weak luminescence due to its lower crystallinity.

The figure 4 shows that the intensity of the luminescence spectra decreases with increasing concentration of the Bi ions. In this case, no modification in the samples structure is detected. When the doped samples were excited with the wavelength at 300 nm, they show intense blue-green luminescence at 485 nm which could be ascribed to the emission band of the Bi^{3+} ion according to the results of Blasse and Bril [11]. The excitation band in the Bi-doped samples corresponds to the $^1S_0 \rightarrow {}^1P_1$ transition, and its blue emission could be ascribed to the $^3P_1 \rightarrow {}^1S_0$ transition.

The figure 5 reveals better the different luminescence behaviour of the Ce-doped HA and Bi-doped HA samples. Thus, the results show that above 15% cerium concentration the area of the peaks increases while in case of Bi-doped HA this area decreases slightly. It can conclude that the samples containing bismuth ions maintain their crystallinity and luminescence properties at higher concentrations and the samples containing cerium ions show a rapid increase of luminescence with a shift from visible to UV zone.

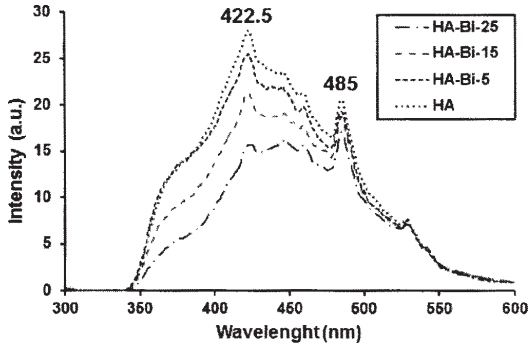

Fig. 4. Emission spectra of the Bi-doped HA at different concentrations

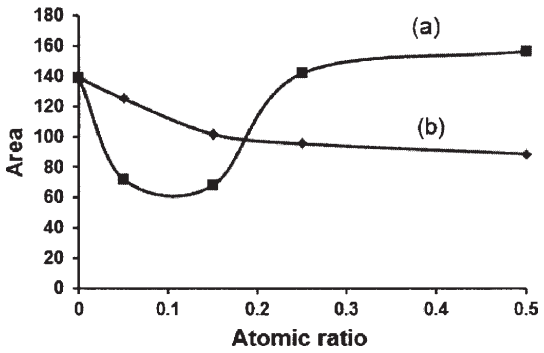

Fig. 5. Peaks Area of the Ce-doped HA (a) and Bi-doped HA (b) samples at different molar ratios of Ce/(Ce+Ca) and Bi/(Bi+Ca)

To the best of our knowledge, this paper demonstrates the obtaining of the Ce-doped and Bi-doped nanocrystalline hydroxyapatite by co-precipitation method at low temperature. Our studies show that the morphology of the nanoparticles does not change with increasing of Ce/(Ca+Ce) and Bi/(Ca+Bi) molar ratios up to 0.15. To elucidate the influence of Ce concentration and Bi concentration on cell functions, drug loading, and release properties, future studies on this topic should be made for the development of materials and the design of bioceramics.

Conclusions

The co-precipitation method has been used for the synthesis of luminescent Ce-doped HA and Bi-doped HA with different concentrations of Ce^{4+} or Bi^{3+}. The emission spectra of the Ce-doped HA and Bi-doped HA give us information about their luminescence properties. It can be seen that the crystallinity of the samples influence the luminescence properties. Thus, if the crystallinity is higher the luminescence intensity is higher. Our data show that the most crystalline is the HA sample. The excitation wavelength is of 300 nm with a very strong emission peak centred at about 422.5 nm for all the samples studied. The

results show that the HA green emission is not improved by Ce^{4+} or Bi^{3+} doping in the hydroxyapatite lattice, but the emission intensity still exist with no modification in the HA structure doped with a concentration of up to 15% Ce^{4+} and Bi^{3+}.

These studies demonstrate that Ce-doped HA and Bi-doped HA are luminescent. They could have potential applications for drug release and targeting based on their luminescent properties.

References

1. MURUGAN, R., RAMAKRISHNA, S., Compos. Sci. Technol., **65**, 2005,p. 2385–2406.
2. HENCH, L.L., POLAK, J.M., Science, **295**, 2002, pp. 1014–1017.
3. STOLERIU, S., IOVAN, G., PANCU, G., GEORGESCU, A., SANDU, A.V., ANDRIAN, S., Mat. Plast., **51**, 2014, p. 162
4. FILIP, L., NEDELCU, I.-A., UNGUREANU, C., SONMEZ, M., ANDRONESCU, E., Rev. Chim. (Bucharest), **65**, 2014, p. 521
5. ALEXANDROAEI, M., IGNAT, M., SANDU, I.G., Rev. Chim. (Bucharest), **64**,no. 10, 2013, p. 1100
6. DOAT, A., PELLE, F., GARDANT N., LEBUGLE, A., J. Solid State Chem., **177**, 2004, p. 1179–1187.
7. BENDREA, A.-D., CIANGA, L., HITRUC, E.-G., TITORENCU, I., CIANGA, I., Mat. Plast., **50**, no. 1, 2013, p. 71
8. CHEN, F., ZHU, P. H., Y.-J., WU, J., ZHANG, C.-L., CUI, D.-X, Biomaterials, **32**, 2011, p. 9031–9039.
9. SHI, D., Adv. Funct. Mater., **19**, 2009, p. 3356–3373.
10. BU¨NZLI, J.-C. G., PIGUET, C., Chem. Soc. Rev., **34**, 2005, p. 1048–1077.
11. BLASSE, G., BRIL, A., J. Chem. Phys., **48**, 1968, p. 217–222.
12. BLASSE, G., MEIJERINK, A., ZUIDEMA, J., J. Phys. Chem. Solids, **55**, 1994, p. 171–174.
13. SANDU, I., POPESCU-CIOCIRLIE, I., GRUIA, I., CALANCIA, O., COSMA, D.G., SANDU, I.G., COZMA, D.G., Rev. Chim. (Bucharest), **49**, no. 11, 1998, p. 756.
14. SANDU, I., POPESCU-CIOCIRLIE, I., GRUIA, I., CALANCIA, O., LIMISCA, G., SANDU, I.G., Rev..Chim. (Bucharest), **49**, no. 10, 1998, p. 673.
15. WEBSTER, T. J., MASSA-SCHLUETER, E. A., SMITH, J. L., SLAMOVICH, E. B., Biomaterials, **25**, 2004, p. 2111-2121.
16. CIOBANU, G., BARGAN, A.M., LUCA, C., Ceramics International, 41, 2015, p. 12192.
17. CIOBANU, G., BARGAN, A.M., LUCA, C., JOM, **67**, 2015, 0. 2534
18. RAYNAUD, S., CHAMPION, E., BERNACHE-ASSOLLANT, D., THOMAS, P., Biomaterials, **23**, 2002, p. 1065–1072.
19. SUN, H.-T., ZHOU, J., QIU, J. Prog. Mater. Sci., **64**, 2014, p. 1–72.
20. ANDRÉA, R.S., PARIS, E.C., GURGEL, M.F.C., ROSA, I.L.V., PAIVA-SANTOS, C.O., LI, M.S., VARELA, J.A., LONGO, E., J. Alloy. Compd., **531**, 2012, p. 50–54

Manuscript received: 21.02.2015